Synthesis and Structure of Some M^{II}/M^{III} Mixed Fluorides with Pyrochlore and Weberite Related Structures

M. A. Subramanian[a], W. J. Marshall[a], R.-D. Hoffmann[b], and A. W. Sleight[c]

[a] Central Research and Development Department, Experimental Station, Wilmington, DE 19880-0328, USA
[b] Institut für Anorganische und Analytische Chemie, Universität Münster, Corrensstraße 30 – 36, D-48149 Münster, Germany
[c] Department of Chemistry, Oregon State University, Corvallis, OR 97331-4003, USA

Reprint requests to Prof. Dr. A. W. Sleight. E-mail: arthur.sleight@oregonstate.edu

Dedicated to Professor Wolfgang Jeitschko on the occasion of his 70th birthday

New $NH_4M^{II}M^{III}F_6$ and $M^{II}M^{III}F_5 \cdot 2H_2O$ compounds with the pyrochlore and weberite structures, respectively, are reported. Structures of NH_4CoCrF_6, $AlZnF_5 \cdot 2H_2O$, and $GaMnF_5 \cdot 2H_2O$ were refined using X-ray diffraction data from single crystals. The structures of $Mg^{II}Al^{III}F_5 \cdot H_2O$ and $NH_4Mg^{II}Al^{III}F_6$ were refined from powder X-ray diffraction data. Magnetic susceptibility data indicates antiferromagnetic ordering in $NH_4Co^{II}V^{III}F_6$ at 7 K but no ordering in $NH_4Co^{II}Cr^{III}F_6$ down to 4.2 K. Electrical conductivity presumably due to protons was observed in $MgAlF_5 \cdot (H_2O)_2$.

Key words: Fluorides, Weberite, Pyrochlore

Introduction

For $A_2M^{II}M^{III}F_7$ and $AM^{II}M^{III}F_6$ compounds with octahedral M^{II} and M^{III} cations, the pyrochlore structure (Fig. 1) is frequently found. Another structure for
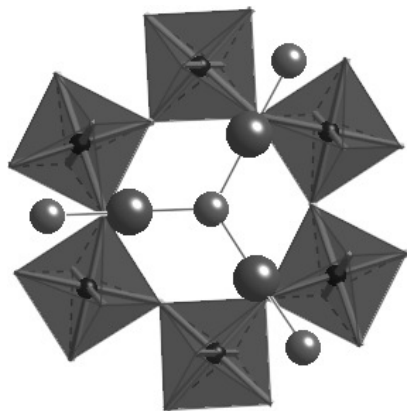

Fig. 1. The $A_2M_2X_6X'$ pyrochlore structure viewed down the [111] axis. The M_2X_6 octahedral network is shown as corner sharing polyhedra. The A cations are the small spheres, and the X' anions are large spheres. The lines between A and X' are on 3-fold axes and define the 32*e* site. In AM_2X_6 pyrochlores the A cation is generally on the X' site but partially delocalized onto the 32*e* site.

$A_2M^{II}M^{III}F_7$ fluorides is the weberite structure. Here the M^{II} and M^{III} cations reside on octahedral sites distinctly different from one another. A variation of this formula for the weberite structure (Fig. 2) is $M^{II}M^{III}F_5 \cdot 2H_2O$. Here two F atoms have been replaced with water molecules, and the A cations are missing. The $M^{II}M^{III}F_5 \cdot 2H_2O$ weberites are known as inverse weberites because for M^{II} and M^{III} the sites are interchanged relative to $A_2M^{II}M^{III}F_7$ weberites.
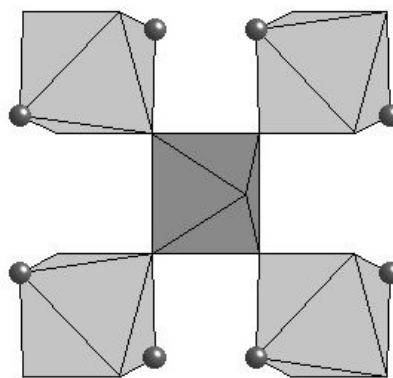

Fig. 2. A fragment of the weberite structure as M^{II} octahedral (light) and M^{III} (dark) octahedral, *z*-axis horizontal and *y*-axis vertical. The spheres are O of H_2O molecules.

Table 1. Unit cell edges for $M^{II}M^{III}F_5 \cdot 2H_2O$ compounds with the Weberite structure.

Compound	a (Å)	b (Å)	c (Å)
$ZnAlF_5 \cdot 2H_2O$	7.141(2)	10.307(4)	6.645(2)
$CoAlF_5 \cdot 2H_2O$	7.193(2)	10.352(4)	6.608(2)
$MnAlF_5 \cdot 2H_2O$	7.229(2)	10.487(4)	6.816(2)
$MgAlF_5 \cdot 2H_2O$	7.057(2)	10.125(4)	6.798(2)
$CdAlF_5 \cdot 2H_2O$	7.331(2)	10.639(4)	6.829(2)
$ZnGaF_5 \cdot 2H_2O$	7.380(2)	10.600(4)	6.584(2)
$MnGaF_5 \cdot 2H_2O$	7.471(2)	10.735(4)	6.720(2)
$CdGaF_5 \cdot 2H_2O$	7.603(2)	10.875(4)	6.718(2)
$ZnVF_5 \cdot 2H_2O$	7.486(2)	10.756(4)	6.589(2)
$MnVF_5 \cdot 2H_2O$	7.607(2)	10.912(4)	6.728(2)

Table 2. Summary of structure refinement of $Zn^{II}Al^{III}F_5 \cdot 2H_2O$.

Space group	*Imma*
a Cell edge	7.141(2) Å
b Cell edge	10.307(4) Å
c Cell edge	6.645(2) Å
Density, calcd.	3.021 g/cm^3
Z	4
Crystal	Colorless prism; 0.057 × 0.64 × 0.10 mm
No. reflections	1407
Data collection temperature	22 °C
Unique reflections with $I \geq 3.0\sigma(I)$	247
2θ Range	6.9° - 50.1°
Maximum h, k, l	12, 8, 7
μ (Mo)	53.44 cm^{-1}
Absorption correction	DIFABS
Range of transmission factors	0.6 – 1.19
Duplicate reflections	236
R merge	2.2%
Al position	$4c : 1/4, 1/4, 1/4$
Mg position	$4b : 0, 1/2, 1/2$
F1 position	$16j : 0.2907(3), 0.3731(2), 0.4357(3)$
F2 position	$4e : 0, 1/4, 0.1833(6)$
O position	$8h : 1/2, 0.5777(5), 0.2160(7)$
H position	$16j : 0.071(7), 0.093(4), 0.655(7)$
B(Al)	0.9(1) Å^2
B(Zn)	1.3(1) Å^2
B(F1)	1.6(1) Å^2
B(F2)	1.3(1) Å^2
B(O)	2.6(1) Å^2
B(H)	4.(1) Å^2
Rw	0.030
R	0.027
Residue electron density peak	0.54 e/Å^3 near Zn

Table 3. Summary of Structure Refinement of $Mn^{II}Ga^{III}F_5 \cdot 2H_2O$.

Space group	*Imma*
a Cell edge	7.471(2) Å
b Cell edge	10.735(4) Å
c Cell edge	6.720(2) Å
Density, calcd.	3.137 g/cm^3
Z	4
Crystal	pink prism; 0.012 × 0.023 × 0.036 mm
No. reflections	1578
Data collection temperature	22 °C
Unique reflections with $I \geq 3.0\sigma(I)$	223
2θ Range	6.6° – 50.1°
Maximum h, k, l	12, 8, 7
μ (Mo)	72.47 cm^{-1}
Absorption correction	None
Duplicate reflections	422
R merge	3.6%
Ga position	$4c: 1/4, 1/4, 1/4$
Mn position	$4b: 0, 1/2, 1/2$
F1 position	$16j: 0.2105(6), 0.3729(4), 0.0597(7)$
F2 position	$4e: 0, 1/4, 0.3179(6)$
O position	$8h: 1/2, 0.425(1), -0.298(2)$
H position	$16j: 0.07(1), 0.095(8), 0.66(1)$
B(Ga)	1.8(1) Å^2
B(Mn)	2.1(1) Å^2
B(F1)	2.5(1) Å^2
B(F2)	2.3(2) Å^2
B(O)	3.5(3) Å^2
B(H)	3.(2) Å^2
Rw	0.051
R	0.052
Residue electron density peak	0.74 e/Å^3 near Mn

In this paper we present results on the synthesis and structure of some $NH_4M^{II}M^{III}F_6$ and $M^{II}M^{III}F_5 \cdot 2H_2O$ compounds with the pyrochlore and weberite structures, respectively. Such compounds have been found to be highly effective catalysts or catalyst precursors for processing halogenated hydrocarbons [1, 2]. When the M^{II} and M^{III} cations are transition metal cations, the $NH_4M^{II}M^{III}F_6$ pyrochlores and the $M^{II}M^{III}F_5 \cdot 2H_2O$ weberites have also been of interest as examples showing magnetic frustration [3].

Experimental Section

Two synthesis procedures used for $M^{II}M^{III}F_5 \cdot 2H_2O$ compounds produced identical results. In one approach, oxides or salts of the M^{II} and M^{III} cations were dissolved in 48% aqueous HF at r. t. in Teflon® containers to give solutions with a 1 : 1 $M^{II} : M^{III}$ ratio. This solution was then evaporated to dryness by heating. In the other approach, 48% aqueous HF was added to a solution of the chlorides of the M^{II} and M^{III} cations. The precipitate formed was washed with distilled water and dried at 110 °C. Single crystals could sometimes be obtained by sealing reactants in Pt tubes and heating to 400 °C under 3 kbars pressure for 2 days.

Table 4. Summary of Structure Refinement of $NH_4Co^{II}Cr^{III}F_6$.

Space group	$Fd3m$
Cell edge	10.297(1) Å
Density, calcd.	3.137 g/cm^3
Z	8
Crystal	green prism; $0.12 \times 0.15 \times 0.24$ mm
No. reflections	1811
Data collection temperature	23 °C
Unique reflections with $I \geq 3.0\sigma(I)$	159
2θ range	$7.9° – 79.7°$
Maximum h, k, l	18, 18, 18
μ (Mo)	72.47/cm
Absorption correction	None
Duplicate reflections	209
R merge	2.0%
Co/Cr position	$16c : 0,0,0$
F position	$48f : x, 1/8, 1/8; x = 0.674(2)$
N position	$8a : 1/8, 1/8, 1/8$
B(Co/Cr)	0.5(1) Å^2
B(Mn)	1.3(1) Å^2
B(N)	6.5(1) Å^2
(Co/Cr) – F	1.9480(7) Å
Rw	0.031
R	0.023
Residue electron density peak	0.72 e/Å^3 near N

Table 5. Selected interatomic distance and angles in $Zn^{II}Al^{III}F_5 \cdot 2H_2O$ and $Mn^{II}Ga^{III}F_5 \cdot 2H_2O$.

$Zn^{II}Al^{III}F_5 \cdot 2H_2O$		$Mn^{II}Ga^{III}F_5 \cdot 2H_2O$	
Zn – F1 × 4	2.003(3) Å	Mn – F1 × 4	2.123(4) Å
Zn – O × 2	2.044(6) Å	Mn – O × 2	2.16(1) Å
Al – F1 × 4	1.787(4) Å	Ga – F1 × 4	1.864(4) Å
Al – F2 × 2	1.850(1) Å	Ga – F2 × 2	1.925(1) Å
O – H × 2	0.67(4) Å	O – H × 2	0.65(7) Å
F1 – Zn – F1	95.4(2)°	F1 – Mn – F1	95.8(2)°
F1 – Zn – F1	84.6(2)°	F1 – Mn – F1	84.2(2)°
F1 – Zn – O	93.2(2)°	F1 – Mn – O	93.6(3)°
F1 – Zn – O	86.8(2)°	F1 – Mn – O	86.4(3)°
F1 – Al – F1	89.9(3)°	F1 – Ga – F1	89.8(3)°
F1 – Al – F1	90.1(3)°	F1 – Ga – F1	90.2(3)°
F1 – Al – F2	89.7(1)°	F1 – Ga – F2	89.4(3)°
F1 – Al – F2	90.3(1)°	F1 – Ga – F2	90.6(3)°
H – O – H	99(9)°	H – O – H	119(19)°

Table 6. Summary of Structure Refinement of $Mg^{II}Al^{III}F_5 \cdot 2H_2O$.

Space group	$Imma$
a Cell edge	7.057(2) Å
b Cell edge	10.125(4) Å
c Cell edge	6.798(2) Å
Al position	$4c$: ¼, ¼, ¼
Mg position	$4b$: 0, ½, ½
F1 position	$16j$: 0.2033(5), 0.3736(4), 0.4295(5)
F2 position	$4e$: 0, ¼, 0.172(1)
O position	$8h$: 0, 0.4126(7), 0.7850(9)
B(Al)	0.4(1)Å^2
B(Mg)	1.5(2)Å^2
B(F1)	0.5(1)Å^2
B(F2)	0.5Å^2
B(O)	0.6(2)Å^2
R_{wp}	9.11
R_p	7.26

X-ray diffraction data were collected on $AlZnF_5 \cdot 2H_2O$ and $GaMnF_5 \cdot 2H_2O$ crystals using a Rigaku RU300 with an R-AXIS image plate detector. An Enraf-Nonius CAD4 diffractometer was used for data collection for the NH_4CoCrF_6 crystal. The structure of $AlZnF_5 \cdot 2H_2O$ was solved by automated Patterson analysis using PHASE. Parameters from $AlZnF_5 \cdot 2H_2O$ were used to initiate a least-squares refinement of $GaMnF_5 \cdot 2H_2O$. The structure of NH_4CoCrF_6 was solved by direct methods using MULTAN.

X-ray diffraction data for Rietveld analysis on $Mg^{II}Al^{III}F_5 \cdot H_2O$ and $NH_4Mg^{II}Al^{III}F_6$ powders were collected with a Siemens D5000 diffractometer using Cu-K$_\alpha$ radiation and a Kevex detector. Data were collected over the 2θ range of 10 to 164°. Refinement of these data utilized RIETAN software.

Results

The unit cell dimensions for compounds prepared with the weberite structure are given in Table 1. These compounds were first revealed in our patent in 1996 [1]. Subsequently, there were reports on $MgAlF_5 \cdot (H_2O)_2$ and $MnVF_5 \cdot (H_2O)_2$ [4, 5] Other compounds known to have the inverse weberite structure are $Fe_2F_5 \cdot (H_2O)_2$, $ZnFeF_5 \cdot 2H_2O$, $MnFeF_5 \cdot 2H_2O$, $Zn^{II}Al^{III}F_5 \cdot 2H_2O$ and $CoFeF_5 \cdot 2H_2O$ [3, 6].

Tables 2–4 summarize the structural analyses of $Zn^{II}Al^{III}F_5 \cdot 2H_2O$ and $Mn^{II}Ga^{III}F_5 \cdot 2H_2O$ based on single crystal X-ray diffraction data. Selected interatomic distances and angles for $Zn^{II}Al^{III}F_5 \cdot 2H_2O$ and $Mn^{II}Ga^{III}F_5 \cdot 2H_2O$ are given in Table 5. Electron density associated with hydrogen atoms could be located for $Zn^{II}Al^{III}F_5 \cdot 2H_2O$ and $Mn^{II}Ga^{III}F_5 \cdot 2H_2O$, but not for $NH_4Co^{II}Cr^{III}F_6$. The structures of $Mg^{II}Al^{III}F_5 \cdot 2H_2O$ and $NH_4Mg^{II}Al^{III}F_6$ were refined from X-ray powder diffraction data. These results are summarized in Tables 6 and 7, and Table 8 gives some interatomic distances and angles for $Mg^{II}Al^{III}F_5 \cdot 2H_2O$. The results in Table 7 for $NH_4Mg^{II}Al^{III}F_6$ actually are based on a model where two hydrogen sites were placed in $32e$ with $x = 0.434$ and $x = 0.316$, each site being 50% occupied. If this hydrogen was not included, agreement factors of $R_{wp} = 7.69$ and R_p of 6.27 were obtained. The compound $NH_4Mg^{II}Al^{III}F_6$ was first

Table 7. Summary of Structure Refinement of $NH_4Mg^{II}Al^{III}F_6$.

Space group	$Fd3m$
Cell edge	9.9608(2) Å
F position	$48f : x, 7/8, 7/8; x = 0.6586(3)$
Mg/Al position	$16c : 0, 0, 0$
N position	$8b : 3/8, 3/8, 3/8$
B(F)	1.6(1) Å^2
B(Mg/Al)	1.1(2) Å^2
B(N)	4.0(7) Å^2
(Mg/Al) – F	1.79 Å
R_{wp}	5.72
R_p	4.44

Table 8. Selected interatomic distances and angles in $Mg^{II}Al^{III}F_5 \cdot 2H_2O$.

|			
Mg – F1 × 4	1.98(1) Å	Mg – O × 2	2.13(1) Å
Al – F1 × 4	1.78(1) Å	Al – F2 × 2	1.84(1) Å
F1 – Mg – F1	92.8(8)°	F1 –Mg – F1	87.2(8)°
F1 – Mg – O	92.8(8)°	F1 – Mg – O	87.2(8)°
F1 – Al – F1	89.4(9)°	F1 – Al – F1	90.3(9)°
F1 – Al – F2	88.9(9)°	F1 – Al – F2	91.1(9)°

reported in 1972 as a cubic phase, but no further structural information was given [7].

The (Mg/Al)-F distance found in $NH_4Mg^{II}Al^{III}F_6$ of 1.79 Å agrees well with the 1.77 Å expected based on Shannon radii. The (Co/Cr)–F distance of 1.95 Å found in $NH_4Co^{II}Cr^{III}F_6$ is reasonable since the expected value based on Shannon radii would be 1.93 Å (based on Co^{II} low-spin) or 1.98 Å (based on Co^{II} high-spin). AC magnetic susceptibility data were obtained in a 1 Oe field at a frequency of 125 Hz over the temperature range 4.2 to 30 K on $NH_4Co^{II}Cr^{III}F_6$ and $NH_4Co^{II}V^{III}F_6$. No magnetic ordering was found in this temperature range for $NH_4Co^{II}Cr^{III}F_6$, but a sharp drop in susceptibility at about 7 K for $NH_4Co^{II}V^{III}F_6$ suggests antiferromagnetic ordering.

Complex impedance data were obtained on $MgAlF_5 \cdot (H_2O)_2$ at r. t. and 323 K as a function of relative humidity (Fig. 3). The observed conductivity is presumably from protons and increases with both temperature and humidity. This conductivity was reversible with respect to both temperature and humidity.

The thermal decomposition of $Mg^{II}Al^{III}F_5 \cdot 2H_2O$ at 250 ℃ yielded a phase giving a pyrochlore-type diffraction pattern with $a = 9.83$ Å. By analogy to the known pyrochlore $Fe_2F_5 \cdot H_2O$ [8], the formula for this pyrochlore is likely $Mg^{II}Al^{III}F_5 \cdot H_2O$.

Two other pyrochlore phases prepared in the course of this work had the presumed formulas $Ca_{1/2}MgAlF_6$
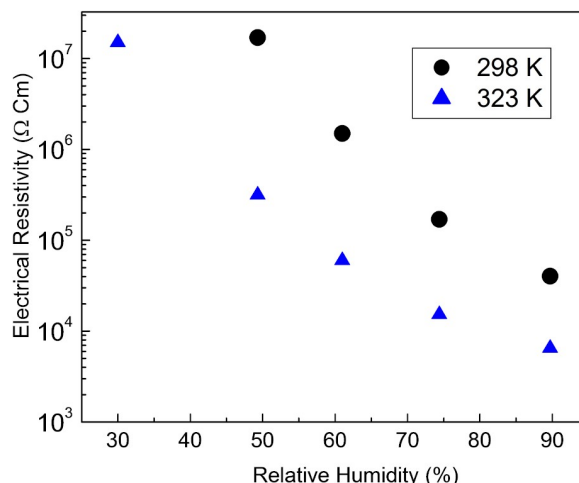
Fig. 3. The electrical resistivity *vs*. humidity for $Mg^{II}Al^{III}F_5 \cdot 2H_2O$ determined through complex impedance spectra.

($a = 10.02$ Å) and $Sr_{1/2}MgAlF_6$ ($a = 0.12$ Å). Both can apparently hydrate as in the case of $KNbWO_6 \cdot xH_2O$.

Discussion

The ideal formula for the pyrochlore structure is $A_2M_2X_6X'$. The backbone of this structure is the M_2X_6 network, and high levels of deficiencies can exist on both the A (16c) and X' (8a) sites. For $AM^{II}M^{III}F_6$ pyrochlores the X' anion is missing, and the one A cation is basically on this "anion" site. High displacement factors for N are observed in $NH_4Fe_2F_6$ (2.5 Å^2) [8], ordered-NH_4CoAlF_6 (2.9 Å^2) [9], disordered-NH_4CoAlF_6 (6.3 Å^2) [9], NH_4CoCrF_6 (6.5 Å^2), and NH_4MgAlF_6 (4.0 Å^2). Not surprisingly, these displacement factors are higher when the M^{II} and M^{III} cations are disordered. High displacement factors for the A cation have also been observed in the $RbCoCrF_6$, $RbNb_2O_5F$, $TlNb_2O_5F$, and $TlTaWO_6$ pyrochlores [10, 11]. In these cases, the authors have attributed these high displacement factors to actual partial displacements off the 8a site into the 32e site (Fig. 1). Electrostatic energy calculations on the potential created by the M_2X_6 network show that the 16c site is a much better cation site than is the 8a site [12]. Factors that may push the A cations to the 8a are the repulsion between the A cations and the fact that the 8a site is larger than the 16c site. It appears, however, that for the AM_2X_6 pyrochlores the A cations in the 8a site tend to partially delocalize into the 32e site, which is the site that connects the 8a and 16c sites (Fig. 1). This is supported by our refinement of NH_4MgAlF_6 where much better agree-

ment factors are obtained when some electron density is placed in the $32e$ site. This suggested A cation delocalization is consistent with the fact that AM_2F_6 pyrochlores are known to be ionic conductors of the A^I cations at r. t. [13].

The pyrochlore $Fe_2F_5 \cdot H_2O$ has been found during the thermal decomposition of weberite $Fe_2F_5 \cdot 2H_2O$ [8]. This $Fe_2F_5 \cdot H_2O$ pyrochlore is not a normal hydrated pyrochlore such as $KNbWO_6 \cdot H_2O$ where the H_2O molecules reside within the M_2X_6 network and can be removed without destruction of the pyrochlore structure. The formula for the pyrochlore $Fe_2F_5 \cdot H_2O$ can be rewritten as $H_2Fe_2F_5O$ to emphasize that O is part of the M_2X_6 network and cannot be removed without destruction of the pyrochlore structure. Likewise, the water in pyrochlore $MgAlF_5 \cdot H_2O$ cannot be removed without destruction of the pyrochlore structure. Ordering of Fe^{II} and Fe^{III} occurs in pyrochlore $NH_4Fe_2F_6$, but not in pyrochlore $H_2Fe_2F_5O$ due the disorder of F and O in the network M_2X_6.

Although a great many $AM^{II}M^{III}F_6$ pyrochlores are known, the M^{II} and M^{III} cations are generally disordered. Only $NH_4Fe^{II}Fe^{III}F_6$ and $NH_4Co^{II}Al^{III}F_6$ have been produced in the pyrochlore structure with ordered M^{II} and M^{III} cations [8, 9]. Ordering of M and M' cations in $A_2MM'X_6$ perovskites can occur while maintaining cubic symmetry, but the ordering of M^{II} and M^{III} cations in the pyrochlore structure necessarily destroys the cubic symmetry. The ordering of M^{II} and M^{III} cations in $NH_4Fe^{II}Fe^{III}F_6$ and $NH_4Co^{II}Al^{III}F_6$ produces an orthorhombic pyrochlore structure. The fact that this ordering can occur is somewhat surprising considering that a charge difference of 2 in $A_2MM'X_6$ perovskites rarely produces complete order of the M^{III}

and M^V cations. The case of $NH_4Fe^{II}Fe^{III}F_6$ is easy to understand because this is a matter only of electron ordering as opposed to ordering of cations of different elements. The order that can be obtained in $NH_4Co^{II}Al^{III}F_6$ is likely related to a size difference between Co^{II} and Al^{III} as well as the small charge difference. For $NH_4Mg^{II}Al^{III}F_6$ the size difference between Mg^{II} and Al^{III} is much less and ordering of these cations was not obtained even with long annealing times. The X-ray scattering powers of Al and Mg are so similar that ordering of these cations cannot be detected based on their scattering powers. However, since ordering of M cations in $AM^{II}M^{III}F_6$ pyrochlores always gives an obvious distortion from cubic symmetry, we can conclude that Al and Mg are not ordered in $NH_4Mg^{II}Al^{III}F_6$.

Proton conductivity in oxides is normally attributed to a mixture of OH^- and O^{2-} species where the proton jumps from one O^{2-} to another O^{2-} or to a mixture of H_3O^+ and H_2O species where the proton jumps between water molecules. It is not obvious how either mechanism would be appropriate for $MgAlF_5 \cdot (H_2O)_2$. A proton conductivity of 10^{-2} S/cm at 353 K has been observed in the pyrochlore $HSbO_3 \cdot xH_2O$ where H_3O^+ species are known to be present [14]. For the pyrochlore $Al(OH)_{1/2}F_{1/2} \cdot xH_2O$ a proton conductivity of 10^{-6} S/cm was observed at 298 K [15]. The intermediate proton conductivity in $MgAlF_5 \cdot (H_2O)_2$ could be associated with an exchange of some F^- to OH^-, and the observed conductivity could be due either to the bulk or to grain boundaries.

[1] V. N. M. Rao, M. A. Subramanian, U.S. Patent No. 5,559,069 (1996).

[2] V. N. M. Rao, M. A. Subramanian, U.S. Patent No. 5,880,315 (1999).

[3] J. M. Greneche, J. Linares, F. Varret, Y. Laligant, G. Férey, J. Magn. Magn. Mater. **73**, 115 (1988).

[4] M. Weil, F. Werner, Monatsh. Chem. **132**, 769 (2001).

[5] F. Leroux, A. Mar, D. Guyomard, Y. Piffard, Comptes Rendus de l'Academie des Sciences, Serie IIb: **320**, 147 (1995).

[6] W. Hall, S. Kim, J. Zubieta, E. G. Walton, D. B. Brown, Inorg. Chem. **16**, 1884 (1977).

[7] A. S. Campbell, J. A. Adams, D. T. Howarth, Clay Minerals **9**, 415 (1972).

[8] G. Férey, M. LeBlank, R. dePape, J. Solid State Chem. **40**, 1 (1981).

[9] M. A. Subramanian, W. J. Marshall, R. L. Harlow, Mater. Res. Bull. **31**, 585 (1996).

[10] J. L. Fourquet, C. Jacoboni, R. dePape, Mater. Res. Bull. **8**, 393 (1973).

[11] C. Michel, B. Raveau, Mater. Res. Bull. **8**, 451 (1973).

[12] J. Pannetier, J. Phys. Chem. Solids **34**, 583 (1973).

[13] A. W. Sleight, J. E. Gulley, T. Berzins, Advances in Chemistry Series, **163**, 195 (1977).

[14] U. Chowdhry, J. R. Barkely, A. D. English, A. W. Sleight, Mater. Res. Bull. **17**, 917 (1982).

[15] J. L. Fourquet, M. Riviere, A. Le Bail, M. Nygrens, J. Gris, Eur. J. Solid State Chem. **25**, 535 (1988).